The Formation of the Kamacite Phase in Metallic Meteorites

J. I. GOLDSTEIN

Goddard Space Flight Center
National Aeronautics and Space Administration, Greenbelt, Maryland

Abstract. To predict the concentration gradients in meteoritic kamacite, the newly determined Fe-Ni phase diagram of Goldstein and Ogilvie was applied and a diffusion analysis was developed. The results of the diffusion analysis show that for cooling rates of about 2×10^{-6} deg/yr the kamacite phase cannot remain in equilibrium at low cooling temperatures and a Ni depletion in the kamacite near the α-γ interface occurs below 450°C. Certain other features of the kamacite phase are predicted: (1) an increasing Ni concentration from the center of the kamacite phase toward the α-γ interface in coarse and medium octahedrites, (2) a variation in the average Ni content of the average kamacite bandwidths with the over-all Ni content of the meteorite, and (3) a similar average composition of kamacite plates of the same width regardless of the over-all Ni content of the parent meteorite. These predictions have been confirmed by electron probe measurements of several metallic meteorites. This study shows that the composition of the kamacite phase in meteorites can be predicted from cooling rates of parent bodies which form at low pressure.

Introduction. The formation of the Widmanstätten pattern in metallic meteorites has recently been discussed by *Goldstein and Ogilvie* [1965a] and by *Wood* [1964]. They showed that the iron meteorites formed under conditions of low pressure and in parent bodies which cooled at a rate of about 1–10 $\times$ 10^{-6} deg/yr. Therefore the 1-atm Fe-Ni phase diagram can be used to describe phase equilibriums in iron meteorites, and the 1-atm diffusion coefficients can be used to describe the mass transport of material through the kamacite and taenite phases in iron meteorites. It is my purpose in this paper to predict the composition variations that would occur in the kamacite phase of metallic meteorites if they had cooled at an average rate of about 2 $\times$ 10^{-6} deg/yr at low pressures and to compare predicted composition variations with measured data.

The Fe-Ni phase diagram. The 1-atm Fe-Ni phase diagram has recently been redetermined by *Goldstein and Ogilive* [1965b] (Figure 1). The Ni solubility in α and γ phase was determined experimentally between 800 and 500°C and calculated theoretically below this temperature. The maximum Ni solubility in kamacite was calculated to occur at about 450°C. The diagram differs from *Owen and Liu*'s [1949] in that the range of Ni solubility in the α phase is larger above 500°C and that the Ni solubility

in α bends back to lower Ni contents above 300°C.

Theory. Small concentration gradients have been measured in the kamacite phase of iron meteorites [*Agrell et al.*, 1963]. This indicates that at some time during the cooling of the meteorite, equilibrium conditions were no longer maintained in the kamacite phase. In other words, at some temperature during cooling the composition of the kamacite could not be maintained at the value given by the phase diagram. This nonequilibrium behavior occurs because not enough Fe and Ni can be transferred across the kamacite phase (i.e., low diffusion rates) to maintain equilibrium within the time available.

To describe this process in more detail, I calculated the largest kamacite plate of half-width W that could remain homogeneous at a temperature T_0. The half-width of the kamacite phase was measured across the phase, perpendicular to the α-γ interface. A certain number of assumptions were made in this calculation: (1) The parent body cools at a rate of 2 $\times$ 10^{-6} deg/yr; (2) the process of homogenization is diffusion controlled; (3) the cooling occurs in a stepwise process; and (4) in each interval of cooling Δt, the homogenization process occurs isothermally at an average temperature T_0.
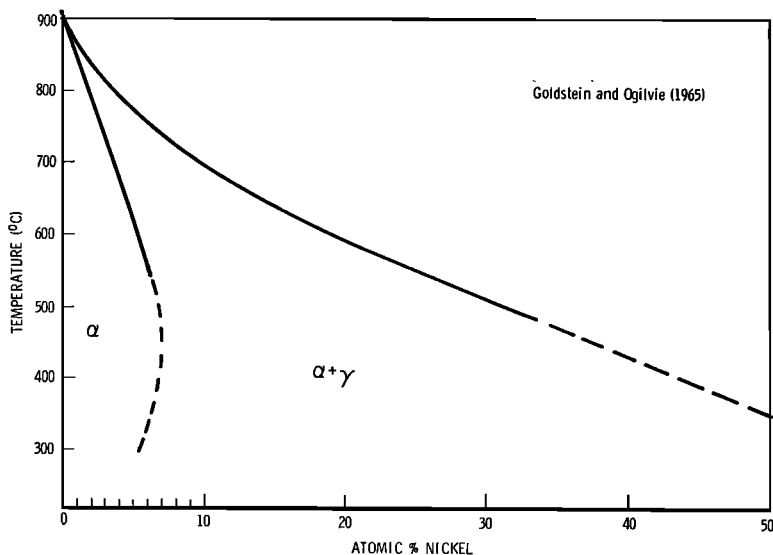
Fig. 1. Fe-Ni phase diagram.

The method of calculation is shown schematically in Figure 2. At time $t = 0$, the kamacite phase is assumed homogeneous at a Ni content C_0 given by the equilibrium phase diagram. From time $t = 0$ to $t = \Delta t$, the equilibrium composition at the kamacite-taenite interface is assumed equal to C_1. During the time increment Δt, the Ni content of the kamacite phase will increase. For the assumed cooling rate and the temperature T_0, the amount to which C, the Ni content at the center of the kamacite phase, approaches C_1 is determined by the diffusion coefficient of mass transport in kamacite D_α. The maximum width W of kamacite for which the degree of homogenization $[(C - C_0)/(C_1 - C_0)]_{\Delta t}$ is equal to some ratio approaching 1 is that width which can still remain homogeneous at temperature T_0. Since D_α is a function of T_0, one can calculate W as a function of temperature.

The interdiffusion coefficients D_α [*Goldstein and Ogilvie*, 1965c], as well as the self-diffusion coefficients $D_{Ni}{}^*$ in α-Fe, have been measured [*Borg and Lai*, 1963]. Good agreement between the interdiffusion measurements [*Goldstein and Ogilvie*, 1965c] and the self-diffusion coefficients of *Borg and Lai* [1963] has been found. The formation of kamacite occurs below the Curie temperature of pure iron. Unfortunately, the activation energy for diffusion has not been measured below this temperature. The excess

activation energy ΔH_x due to the magnetic effect increases the activation energy for diffusion, ΔH. From the calculation of Borg and Lai for ΔH_x, 2.4 kcal, and their measurement of ΔH above the Curie temperature, 61.9 kcal, the value of D_α is estimated and given by

$$D_\alpha = 9.9 e^{-64,300/RT_0} \qquad (1)$$

The values of D_α, extrapolated to as low a temperature as 350°C, are accurate to $\pm 25\%$.

The degree of homogenization and the time interval Δt used for the calculation are interrelated because the difference $C_1 - C_0$ depends on the value of Δt. Calculations were made for two different criteria of homogeneity, a difference of 0.01 and 0.03 atomic % Ni between the center of kamacite and the α-γ boundary. If a value of Δt is used, corresponding to a time period for 25°C of cooling, the degree of homogenization $[(C - C_0)/(C_1 - C_0)]_{\Delta t}$ at 600°C corresponds to 0.97 and 0.90, respectively. W, D_α, and $[(C - C_0)/(C_1 - C_0)]_{\Delta t}$ are related by the following equation [*Crank*, 1956]:

$$\left[\frac{C - C_0}{C_1 - C_0}\right]_{\Delta t} = 1 - \frac{4}{\pi} \sum_{n=0}^{\infty} \frac{(-1)^n}{2n+1}$$

$$\cdot \exp - \left[\frac{D_\alpha(2n+1)^2\pi^2\Delta t}{4W^2}\right]\frac{\cos(2n+1)\pi x}{2W} \qquad (2)$$

where x is the distance from the center of the

kamacite phase (Figure 2). Curves of $[(C - C_0)/(C_1 - C_0)]_{\Delta t}$ are plotted versus x/W for constant values of $D_a \Delta t/W^2$ in Figure 4.1 of *Crank* [1956]. Using the curves given by Crank for $x/W = 0$, we get $W = (D_a\Delta t/1.5)^{1/2}$ and $W = (D_a\Delta t)^{1/2}$ for the two degrees of homogenization, 0.97 and 0.90, respectively, at 600°C. Using the same criteria of homogeneity and a value of Δt corresponding to 25°C of cooling, we get substantially the same equations for W at other temperatures. Figure 3 shows the results of these calculations; the largest kamacite plate of half-width W that can remain homogeneous at a given temperature is plotted versus temperature.

In any metallic meteorite there is a distribution of kamacite bandwidths that usually range from micron to millimeter size. The distribution of bandwidths shows a maximum in a small range of kamacite band sizes (usually the largest-sized bands). It is bands of this general size that compose the Widmanstätten pattern in octahedrites. The average of this small range of band sizes is designated as the average kamacite bandwidth of the meteorite and is usually used in classifying the octahedral structure of the meteorite.
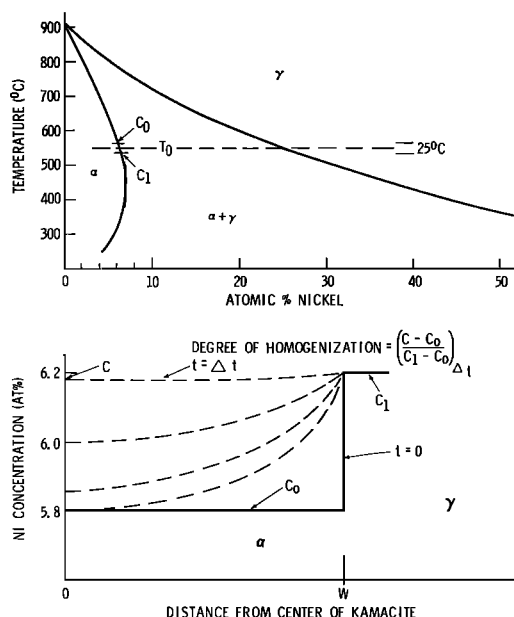
The average kamacite bandwidth and the over-all Ni composition of the meteorite are related. Generally, as the over-all Ni content increases, the size of the average kamacite bands decreases. Table 1 classifies octahedrites roughly according to the size of their kamacite bands.

TABLE 1. Classification of Iron Meteorites

Class	Range of the Average Kamacite Bandwidths, mm	Range of the Ni Content of the Meteorite, wt.% Ni
Hexahedrites (H)	All kamacite	5.5– 6.0
Coarse Octahedrites (Og)	>2	6.0– 7.3
Medium Octahedrites (Om)	0.50–2.0	7.3–10.0
Fine Octahedrites (Of)	0.05–0.50	<17
Ataxites (Ni-rich), plessite (A)	<0.05	<30

This table is taken in a shortened form from *Short and Anderson* [1965]. It emphasizes the fact that the lower boundary limits of the fine octahedrites and ataxites are not well de-

Fig. 2. Schematic of the diffusion analysis used to determine the largest kamacite bandwidth that can remain homogeneous at a given temperature.
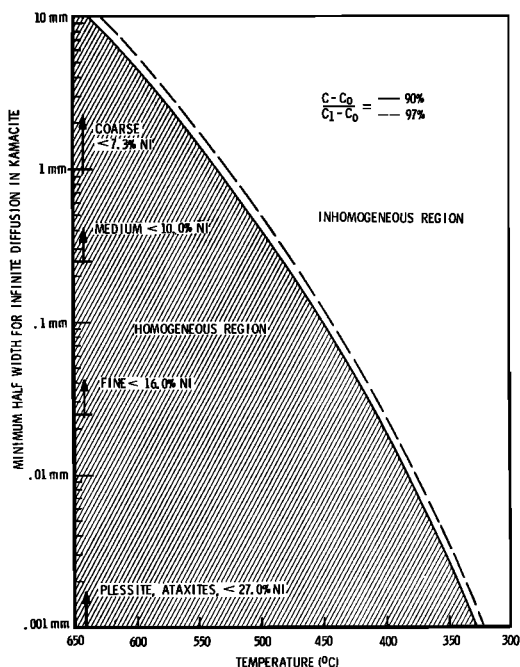

Fig. 3. Minimum half-width for infinite diffusion in kamacite versus cooling temperature.

fined and extend to Ni concentrations for medium and coarse octahedrites. Therefore the classification system given in Table 1 is to be preferred to the one given by *Mason* [1962], which is probably too restrictive.

The results of the diffusion calculations show that inhomogeneity begins at higher temperatures in the thicker kamacite bands. This is due simply to the longer distance through which Ni must diffuse to maintain homogeneity. According to the results of the calculations, kamacite phases in meteorites which have a typical coarse structure remain homogeneous to about 525°C. Meteorites which have a typical medium and fine structure remain homogeneous to about 475 and 400°C, respectively. The kamacite phase in ataxites remains homogeneous below 400°C. In general, the typical fine octahedrites and ataxites remain homogeneous to a temperature below 450°C, the temperature at which the maximum Ni solubility in kamacite occurs; the typical coarse and medium octahedrites become inhomogeneous above 450°C.

From the results of the homogeneity calculations certain predictions about the resultant composition gradients (Figure 4) can be made. These predictions can most easily be discussed by considering the following cases.

Case 1. Average kamacite bandwidths (<0.1 *mm half-width*), *fine octahedrites, ataxites, and plessite.* For kamacite bands which remain homogeneous below 450°C, with a half-width less than 0.1 mm, the Ni concentartion in kamacite should vary in the following manner (Figure 4): At T_3 the bands have reached a maximum Ni content and are homogeneous. At T_4 they are homogeneous and have a lower Ni content, as given by the phase diagram. At T_5, D_a is so low that Ni cannot diffuse completely from the interior of the kamacite phase to the kamacite-taenite interface. This effect produces a Ni depletion in the kamacite phase near the kamacite-taenite interface.

One can also predict that, as the half-width W of kamacite decreases, the average Ni content in kamacite will decrease. In other words, the
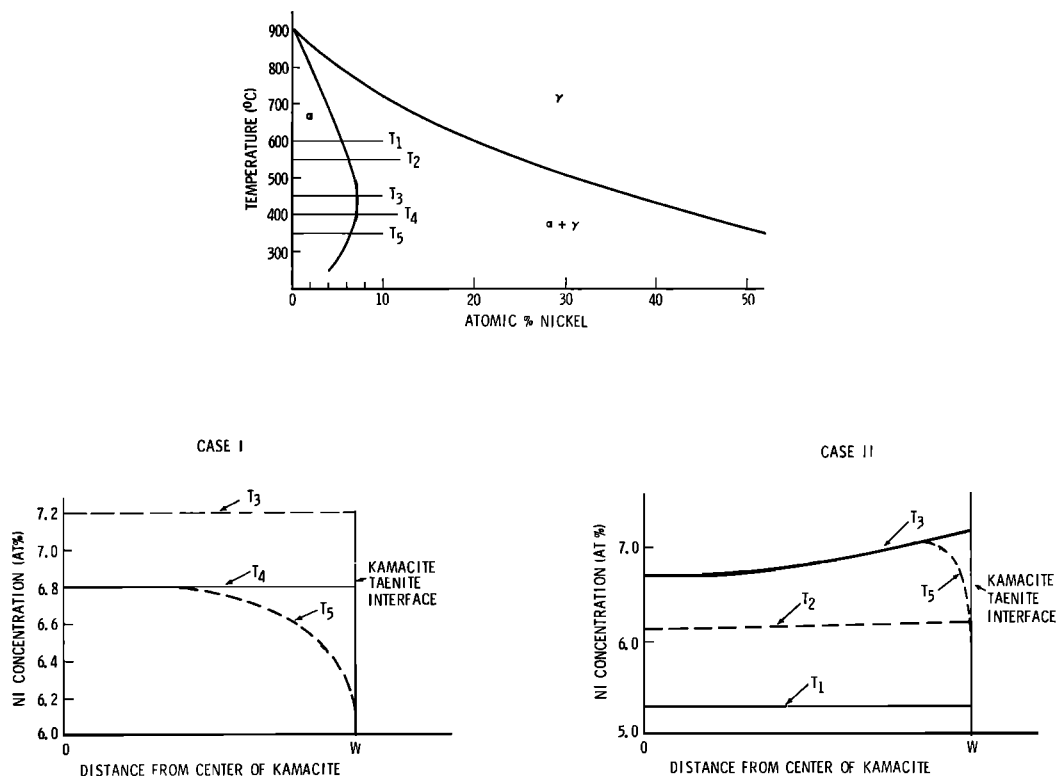

Fig. 4. Predictions of composition variations. Case 1, fine octahedrites, ataxites, and plessite; case 2, coarse and medium octahedrites.

average kamacite bandwidth of the ataxites will have lower Ni contents than the average kamacite bandwidth in fine octahedrites. Also, all kamacite plates of half-width W will have the concentration variation and average Ni content regardless of their origin.

Case 2. Average kamacite bandwidths (> 0.1 mm half-width), coarse and medium octahedrites. For kamacite bands which become inhomogeneous above 450°C, the Ni concentration in kamacite should vary in the following manner (Figure 4): At T_1 the bands are homogeneous, with a Ni content given by the equilibrium phase diagram. At T_2 the Ni content as given by the phase diagram must increase. However, the diffusion coefficient is so low that Ni cannot diffuse completely from the kamacite-taenite interface into the interior of the phase, and a Ni gradient occurs. At T_3 the gradient becomes much larger. Below 450°C, the Ni content at the kamacite-taenite interface begins to decrease. Because of this decrease, a Ni depletion near the α-γ interface forms. The same type of depletion was predicted for the fine octahedrites and the ataxites. Therefore, a gradient occurs near the α-γ interface, as well as the reverse gradient from the center of kamacite towards the α-γ interface. The resultant gradient at temperature T_5 is shown in Figure 4. The reverse gradient, which is predicted to occur, has never been reported.

One can further predict that, as the half-width W of the kamacite phase decreases, the average Ni content in kamacite will increase. This occurs because the smaller-sized kamacite plates remain homogeneous at lower temperatures. Combining the above prediction with the prediction made for case 1, namely, that as the kamacite width decreases the average Ni content decreases, the following relation is predicted: as the width of the average kamacite bandwidth decreases from the millimeter size to the micron size, the average Ni content of the kamacite will increase, going from coarse to medium octahedrites (7% to approximately 10% Ni), and will then begin to decrease from the fine octahedrites to the ataxites (greater than about 10% Ni). We can also predict that any kamacite plate of half-width W will have the same concentration variation and average composition regardless of its origin.

Experimental procedure. Eight meteorites were analyzed with the electron probe. The meteorites and their average Ni contents are listed in Table 2.

Selected sections of these meteorites were first mounted in bakelite. Before electron-probe microanalysis, the samples were polished with $\frac{1}{4}$-μ diamond paste, special care being taken to make sure that there were no apparent height differences between the α and γ phases. The orientation of the kamacite plates that were analyzed was not determined.

An Applied Research Laboratories electron microanalyzer was used to measure the Ni concentrations across the kamacite phases of the meteorites. In making the measurements two important factors were considered: (1) accuracy—accurate measurement of the true composition of kamacite; (2) precision—precise measurement of the differences in composition from one point to another in the kamacite phase.

To measure the absolute kamacite composition accurately, we used well-analyzed Fe-Ni standards. The alloys and the use of these standards has been described by *Goldstein et al.* [1965]. A precision of better than 10% of the amount present can be obtained only if, the X-ray intensity is measured quantitatively.

TABLE 2. Meteorites Analyzed in This Study

Meteorite	Average Ni Content, wt. %	Classification	Reference
Smithsonia	5.88	H	*Roy and Wyant* [1950]
Canyon Diablo	7.18	Og	*Lovering et al.* [1957]
Carbo	8.68	Om	*Palache and Gonyer* [1930]
Breece	9.17	Om	*Henderson and Perry* [1958]
Mount Edith	9.40	Om	*Lovering et al.* [1957]
Carlton	12.77	Of	Henderson, private communication
Dayton	18.10	A	*Henderson and Perry* [1958]
Weaver Mountains	18.03	A	*Henderson and Perry* [1951]

In this study long counting times were necessary. At least 100,000 counts of Ni were measured, ensuring that a variation of better than 1% of the amount present at any one point in the kamacite phase could be measured (3σ about 0.05 wt. % Ni). Allowing for the usual instabilities of the electron probe, we find that a more reasonable estimate of precision is about 0.1 wt. % Ni. The beam stability was checked after every analysis of a kamacite band. If the X-ray intensity varied by more than 2% from the standards, the data were rejected.

The average composition of a kamacite band was computed by (1) taking an average of a point to point analysis, across the phase; (2) taking an average of only a few random points within the phase. Although a complete gradient should be measured, it is estimated by com-
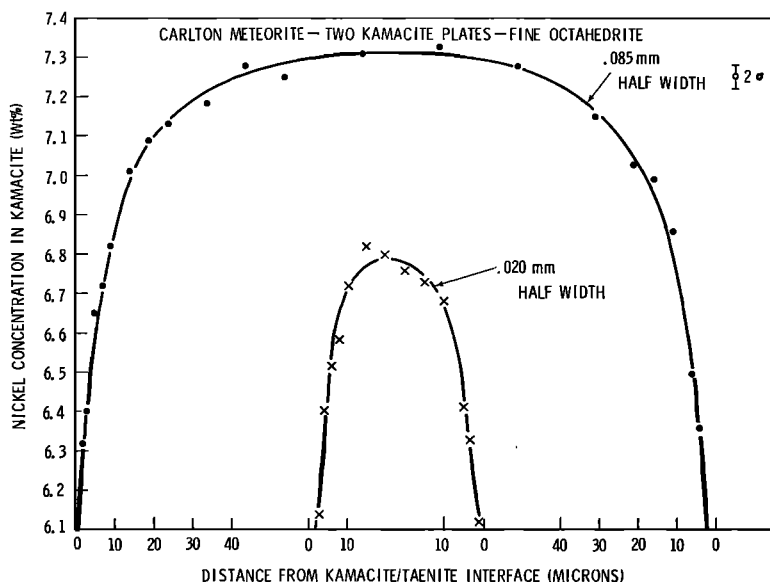
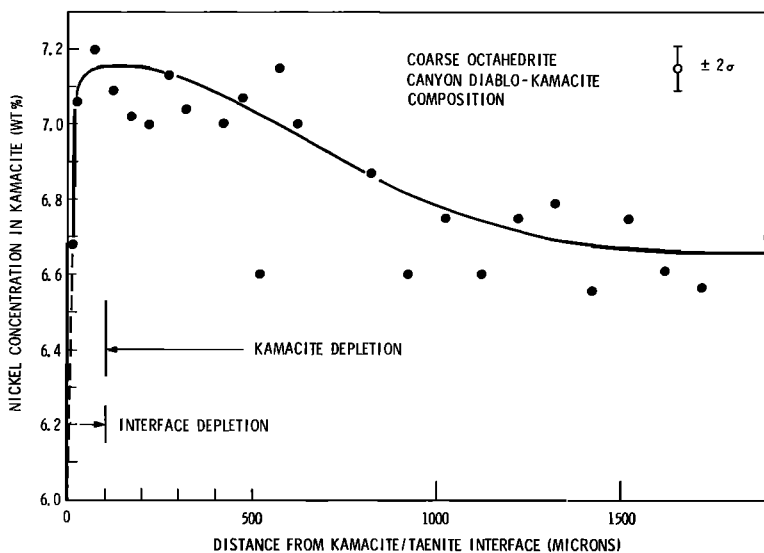Fig. 5.   Ni concentration in the kamacite phase of the Carlton meteorite.

Fig. 6.   Ni concentration in the kamacite phase of the Canyon Diablo meteorite.
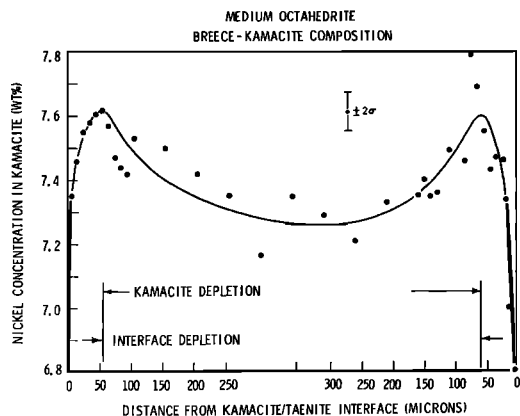
MEDIUM OCTAHEDRITE
BREECE-KAMACITE COMPOSITION

Fig. 7. Ni concentration in the kamacite phase
of the Breece meteorite.

as the half-width decreases from 0.085 to 0.020 mm. This variation was also predicted as a result of the diffusion model.

Several electron probe scans were made across kamacite bands having half-widths greater than 0.1 mm (case 2). A scan across a kamacite band in the Canyon Diablo coarse octahedrite is shown in Figure 6, and a scan across a kamacite band in the Breece medium octahedrite is shown in Figure 7. Both scans show the reverse gradient from the center of the kamacite phase toward the α-γ interface and the interface depletion, starting 50 μ from the interface. From these two figures we see that the average kamacite composition, as predicted, increases for the average kamacite bandwidths from the coarse to the medium octahedrites.

Measurements of the average composition of averaged kamacite bandwidths were made for the eight meteorites studied. The averaging technique has been described. These measurements and the measurements of *Reed* [1965] and *Short and Anderson* [1965] are plotted versus the over-all Ni concentration of the meteorite (Figure 8). These authors did not include the Ni depletion near the α-γ interface in their averaging process. Therefore their averaging process will yield average Ni concentra-

parison with measured bands of comparable size that an average of only a few measurements will still yield a value of the average Ni content accurate to 0.25 wt. % Ni.

Results. Several electron probe scans were made across kamacite bands having half-widths of less than 0.1 mm (case 1). Typical scans across two kamacite bands in the Carlton fine octahedrite are shown in Figure 5. The predicted Ni gradients for case 1 are verified. The average composition of the kamacite decreases

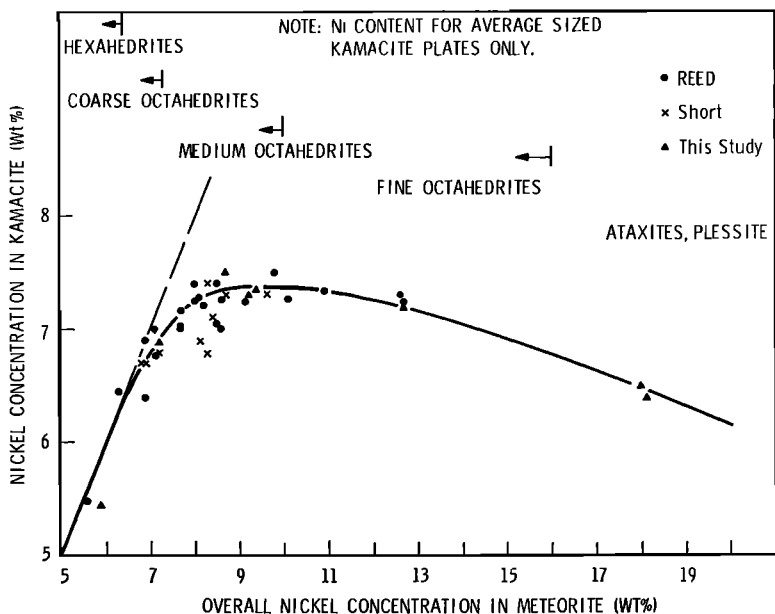
Fig. 8. Variation of Ni concentration in kamacite with the over-all Ni content of the meteorite.

6230   J. I. GOLDSTEIN

tions slightly higher than those obtained in this study. The experimental data verify the prediction that the kamacite composition will increase from coarse to medium octahedrites (7 to approximately 10% Ni) and will then begin to decrease from the fine octahedrites to the ataxites (greater than about 10% Ni).

The composition of kamacite bands smaller than the average kamacite bandwidths of the meteorite was measured. The results of these analyses are shown in Figure 9, where the average Ni content of the kamacite phase is plotted as a function of the width of the phase. A band is drawn through the data points. The bandwidth represents the uncertainty in the orientation of the kamacite phase with respect to the polished surface and the uncertainty in the

measurement of the average Ni content in kamacite. In the Canyon Diablo meteorite, for example, as the size of the kamacite phase decreases from that of the average bandwidth (> 1 mm) the average nickel content in kamacite increases and then decreases. In the Carlton meteorite, as the size of the kamacite phase decreases from that of the average-sized band (about 0.1 mm) the average Ni content in the kamacite decreases. For kamacite bands characterized by a half-width W, the average composition of the phase is the same regardless of the over-all Ni content of the parent meteorite. This result confirms another prediction that resulted from the diffusion model.

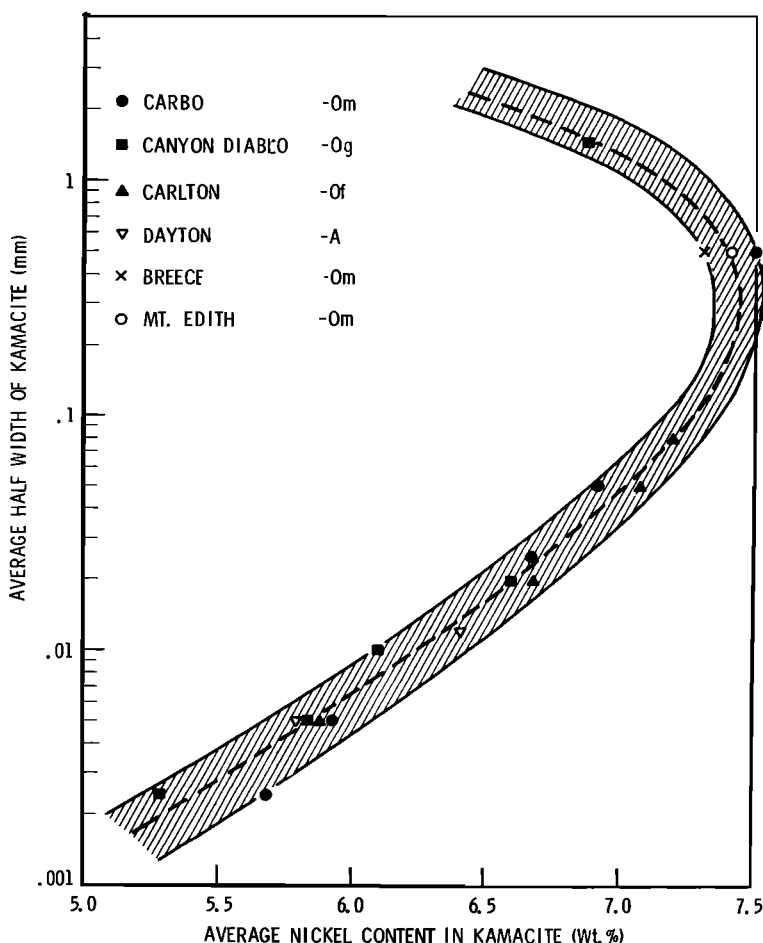*Discussion.* The interface depletion in the kamacite phase can now be explained on the

Fig 9. Average Ni concentration in kamacite versus the average half-width of kamacite for several meteorites.

basis of the newly determined Fe-Ni diagram [*Goldstein and Ogilvie*, 1965*b*]. The prediction of a Ni enrichment from the center of the kamacite phase extending close to the α-γ interface for coarse and medium octahedrites has been verified. This is the first report of such a gradient. An explanation has been given of the variation of the average Ni content of kamacite plates of varying sizes within one meteorite, first reported by *Short and Anderson* [1965].

The nickel content of the kamacite phase is not constant. Even if one neglects the interface depletion in kamacite, the kamacite phase is still not homogeneous. Therefore, the only place where equilibrium conditions exist in metallic meteorites at low temperatures is at the kamacite-taenite interface. The values of the kamacite and taenite compositions at the kamacite-taenite interface [*Reed*, 1965] are in substantial agreement with the solubility limits of the new Fe-Ni phase diagram at about 350°C.

The diffusion analysis that was used in this study is based on a number of approximations that limit its accuracy. It does not allow us to estimate the absolute amount of the Ni concentration gradients or their extent. The electron probe data for the meteorites analyzed in this study are consistent with the predicted concentration gradients based on a cooling rate of the order of 1–10×10^{-6} deg/yr. This assumed cooling rate is in agreement with a theory of origin by which metallic meteorites are formed either in one or several parent asteroidal bodies 100 to 250 km in radius or in isolated metallic areas in a larger parent body cooling at this rate. The results of this investigation provide further evidence for the low-pressure origin of meteorites.

Conclusions. On the basis of a diffusion model and the newly determined Fe-Ni phase diagram, the following predictions about the kamacite phase in meteorites are made.

1. The kamacite phase becomes inhomogeneous during the cooling process.

2. A Ni depletion near the α-γ interface forms below 450°C.

3. A concentration gradient from the center of the kamacite phase toward the α-γ interface forms in the typical-sized kamacite plates of coarse and medium octahedrites.

4. A variation in the average Ni content of typical kamacite bandwidths occurs with the over-all Ni content of the meteorite.

5. The average composition of kamacite plates of the same width is the same regardless of the over-all Ni content of the parent meteorite.

These predictions have been confirmed by electron probe measurements of several metallic meteorites. This correlation is consistent with cooling rates of parent bodies which form at low pressures.

REFERENCES

Agrell, S. O., J. V. P. Long, and R. E. Ogilvie, Nickel content of kamacite near the interface with taenite in iron meteorites, *Nature*, *198*(4882), 749–750, 1963.

Borg, R. J., and D. Y. F. Lai, The diffusion of gold, nickel, and cobalt in alpha iron: A study of the effect of ferromagnetism upon diffusion, *Acta Met.*, *11*, 861–866, 1963.

Crank, J., *The Mathematics of Diffusion*, pp. 45–46, Oxford University Press, London, 1956.

Goldstein, J. I., and R. E. Ogilvie, The growth of the Widmanstätten pattern in metallic meteorites, *Geochim. Cosmochim. Acta*, *29*, 893–920, 1965*a*.

Goldstein, J. I., and R. E. Ogilvie, A reevaluation of the Fe-rich portion of the Fe-Ni system, *Trans. AIME,* to be published, 1965*b*.

Goldstein, J. I., R. E. Hanneman, and R. E. Ogilvie, Diffusion in the Fe-Ni system at 1 atm. and 40 kbar pressure, *Trans. AIME, 233*, 812–820, 1965.

Henderson, E. P., and S. H. Perry, A reinvestigation of the Weaver Mountains, Arizona, meteorite, *Popular Astron., 59*, 263, 1951.

Henderson, E. P., and S. H. Perry, Studies of seven siderites, *Proc. U. S. Natl. Museum, 107*, 339–403, 1958.

Lovering, J. F., W. Nichiporuk, A. Chodos, and H. Brown, The distribution of gallium, germanium, cobalt, chromium, and copper in iron and stony iron meteorites in relation to nickel content and structure, *Geochim. Cosmochim. Acta, 11*, 263–278, 1957.

Mason, B., *Meteorites,* p. 139, John Wiley & Sons, New York, 1962.

Owen, E. A., and Y. H. Liu, Further X-ray study of the equilibrium diagram of the iron-nickel system, *J. Iron Steel Inst. London, 163*, 132–137, 1949.

Palache, C., and F. A. Gonyer, A new iron meteorite from Carbo, Mexico, *Am. Mineralogist, 15*, 388, 1930.

J. I. GOLDSTEIN

Reed, S. J. B., Electron-probe microanalysis of the metallic phases in iron meteorites, *Geochim. Cosmochim. Acta, 29,* 535–549, 1965.

Roy, S. K., and R. K. Wyant, The Mapleton meteorite, *Geol. Ser. Field Museum Nat. Hist., 7,* 129, 1950.

Short, J. M., and C. A. Anderson, Electron microprobe analyses of the Widmanstätten structure of nine iron meteorites, *J. Geophys. Res., 70,* 3745–3759, 1965.

Wood, J. A., The cooling rates and parent planets of several iron meteorites, *Icarus, 3,* 429–459, 1964.